

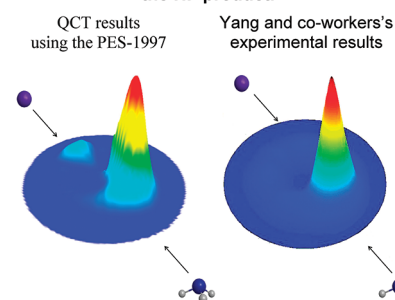
Theoretical Study of the $F + NH_3$ and $F + ND_3$ Reactions: Mechanism and Comparison with Experiment

J. Espinosa-García* and M. Monge-Palacios

Departamento de Química Física, Universidad de Extremadura 06071 Badajoz, Spain

ABSTRACT: We study the barrierless and highly exothermic $F + NH_3$ and $F + ND_3$ abstraction reactions using quasiclassical trajectory calculations based on an analytical potential energy surface developed in our research group. The calculations correctly reproduce the experimental evidence that the vibrational fraction deposited into the DF product for the $F + ND_3$ reaction is greater than into HF for the $F + NH_3$ reaction and that the vibrational distribution is inverted in the $HF(v')$ and the $DF(v')$ products. Of special interest is that recent crossed-beam experiments reported by Yang and co-workers at $4.5 \text{ kcal mol}^{-1}$ are reproduced for both reactions, with a mainly forward symmetry associated with direct trajectories, and a small sideways—backward symmetry contribution associated with “nearly trapped” trajectories due to a “yo-yo” mechanism, different from the previously suggested mechanism of a long-lived complex.

Polar scattering three-dimensional surface plot of the CM scattering angle-velocity distribution for the HF product.



1. INTRODUCTION

Recently Yang and co-workers¹ reported a joint theoretical and experimental study on the title reactions. The theory was a high-level ab initio calculation of the reaction energetics, and the experiment was a crossed-beam study using the universal crossed-beam technique. They found that the dynamics of the reactions of the F atom with NH_3 and ND_3 is essentially the same. The HF and DF products show forward-scattered distributions associated with a direct abstraction mechanism at large impact parameters, with a minor sideways—backward scattering distribution for which a long-lived complex formation mechanism was conjectured. However, those authors reported neither the individual contributions of the two mechanisms nor the individual contribution of the different vibrational states in the products, $HF(v')$ or $DF(v')$.

The title reactions are typical cases of polyatomic hydrogen abstraction reactions. They correspond to barrierless reactions of high exothermicity, permitting the population of excited vibrational states in the products. Such reactions are difficult to study experimentally, because they are not only fast reactions themselves, but they are followed by extremely fast secondary atom/radical reactions.

Theoretically, the accuracy of the dynamics description of a chemical reaction depends mainly on two factors: the dynamics method used, and the potential energy surface (PES) available. In the case of polyatomic systems, quasiclassical trajectory (QCT) calculations have traditionally been the method of choice to study reaction dynamics. Knowledge of the PES plays a crucial role in the study of the dynamics. For the title reactions, only one surface has been proposed. This was in 1997 when our group² reported the first analytical surface with no saddle-point for this reaction, PES-1997. This is basically a valence-bond molecular mechanics (VB-MM) surface with adjustable parameters. It

presents high exothermicity, $-25.80 \text{ kcal mol}^{-1}$, in excellent agreement with recent high-level ab initio calculations,¹ $-25.77 \text{ kcal mol}^{-1}$. In addition, it presents an $H_2N \cdots HF$ hydrogen bond complex in the exit channel, stabilized by $6.25 \text{ kcal mol}^{-1}$ with respect to the products, in relatively good agreement with high-level ab initio calculations,¹ $9.94 \text{ kcal mol}^{-1}$, given the semiempirical character of the PES.

To shed more light on the dynamics of the title reactions and the suggested mechanisms, we performed QCT calculations on the analytical potential energy surface PES-1997. In section 2, a detailed description of the PES and the fitting procedure is presented. In section 3, we briefly outline some computational details of the dynamics calculations. The QCT results are presented in section 4 and compared with the available experimental data. Finally, section 5 contains the conclusions.

2. POTENTIAL ENERGY SURFACE

The analytical PES function we employ is basically a VB-MM surface, given by the sum of three terms: a stretching potential, V_{stretch} , a harmonic bending term, V_{harm} , and an anharmonic out-of-plane potential, V_{op}

$$V = V_{\text{stretch}} + V_{\text{harm}} + V_{\text{op}} \quad (1)$$

It was designed to describe exclusively the hydrogen abstraction reaction.

Received: August 30, 2011

Revised: October 27, 2011

Published: October 27, 2011

The stretching potential is the sum of three London–Eyring–Polanyi (LEP) terms, each one corresponding to a permutation of the three ammonia hydrogens

$$V_{\text{stretch}} = \sum_{i=1}^3 V_3(R_{\text{NH}_i}, R_{\text{NF}}, R_{\text{HF}}) \quad (2)$$

where R is the distance between the two subscript atoms and H_i stands for one of the three ammonia hydrogens. Note that there are 12 fitting parameters, four for each of the three kinds of bond, R_{NH_i} , R_{NF} , and R_{HF} . In particular, these are the singlet and triplet dissociation energies, D_{XY}^1 and D_{XY}^3 , the equilibrium bond distance, R_{XY}^e , and the Morse parameter, α_{XY} , which is allowed to relax from ammonia to the amidogen radical using a switching function that depends on two additional parameters, a and b . Therefore, 14 parameters are required to describe the stretching potential.

The V_{harm} term is the sum of three harmonic terms, one for each bond angle in ammonia

$$V_{\text{harm}} = \frac{1}{2} \sum_{i=1}^2 \sum_{j=i+1}^3 k_{ij}^0 k_i k_j (\theta_{ij} - \theta_{ij}^0)^2 \quad (3)$$

where k_{ij}^0 and k_i are force constants, and θ_{ij}^0 are the reference angles. The k_{ij}^0 force constants are allowed to evolve from their value in ammonia, k^{NH_3} , to their value in the amidogen radical, k^{NH_2} , corresponding to two parameters of the fit, by means of switching functions. In total, 16 parameters need to be fitted for the calibration of the V_{harm} potential.

The V_{op} potential is a quadratic-quartic term whose aim is to correctly describe the out-of-plane motion of ammonia³

$$V_{\text{op}} = \sum_{i=1}^3 f_{\Delta_i} \sum_{\substack{j=1 \\ j \neq i}}^3 (\Delta_{ij})^2 + \sum_{i=1}^3 h_{\Delta_i} \sum_{\substack{j=1 \\ j \neq i}}^3 (\Delta_{ij})^4 \quad (4)$$

The force constants, f_{Δ_i} and h_{Δ_i} , have been incorporated into a switching function which is such that V_{op} vanishes at the amidogen radical limit. Δ_{ij} is the angle that measures the deviation from the reference angle

$$\Delta_{ij} = \text{acos} \left(\frac{\vec{N}_i \cdot \vec{r}_j}{\|\vec{r}_j\|} \right) - \theta_{ij}^0 \quad (5)$$

where N_i is a unit vector normal to the plane defined by the three hydrogen atoms of the ammonia and θ_{ij}^0 is the reference angle. The vector N_i is given by

$$\vec{N}_i = \frac{(\vec{r}_k - \vec{r}_j) \times (\vec{r}_l - \vec{r}_j)}{\|(\vec{r}_k - \vec{r}_j) \times (\vec{r}_l - \vec{r}_j)\|} \quad i = 1, 2, 3 \quad (6)$$

where \vec{r}_j , \vec{r}_k , and \vec{r}_l are vectors going from the nitrogen atom to the j , k , and l hydrogen atoms, respectively, in ammonia. To correctly calculate Δ_{ij} , the motion from j to l has to be clockwise. In total, 4 parameters need to be fitted for the calibration of the V_{op} potential.

Note that in the original expression, the V_{op} term was added to obtain a correct description of the umbrella mode of ammonia.

Although recently Yang and Corchado⁴ noted that this term yields nonphysical behavior along the ammonia inversion path (which was not taken into account originally), this problem is of no importance in the present case because only the hydrogen abstraction reaction is being considered.

The PES-1997 is symmetric with respect to the permutation of the three equivalent ammonia hydrogens, a feature which is especially important in dynamics calculations. It depends on 34 parameters: 14 for the stretching, 16 for the harmonic term, and 4 for the out-of-plane potential. These 34 parameters endow the PES with great flexibility, while keeping the VB/MM functional form physically intuitive.

Once the functional form was available, the 34 parameters describing the PES-1997 were fitted by using as input information a combination of theoretical and experimental data. In this sense therefore, the surface is semiempirical. As theoretical information we used ab initio information (geometry, vibrational frequency, and reaction energy) of reactants, products, and the hydrogen bond complex in the exit channel, $\text{NH}_2 \cdots \text{FH}$. As experimental data input, we used reactant and product properties. Note that this very exothermic ($-25.80 \text{ kcal mol}^{-1}$)² and very fast hydrogen abstraction reaction evolves with no saddle point. Thus, in this case, the ab initio information of this stationary point can not be used in the calibration process. Since one needs some reference information along the reaction path to fit some of the parameters of the surface, we took as reference data the absence of a saddle point and the properties of a stationary point found on the reaction path—the hydrogen bonded complex linking the HF molecule and the NH_2 radical.

For this reaction with no saddle point, we calculated the reaction path starting from a local cubic approach⁵ from reactants separated by several distances up to 9 Å and then going down the steepest descent path using the Page and McIver method,^{5,6} until coming close to the well. Since the well is a stationary point, the gradients along the reaction path become very small as it is approached, causing instabilities in the methods used for the reaction path calculation. Nevertheless, the properties of the last points calculated along the reaction path showed us that it leads from the reactants to the hydrogen-bonded well. Several trials were made with reaction paths starting with different distances between reactants. The final results to be presented in this paper are independent of further increases in the starting distance. For a reaction path without a saddle point, the usual reaction coordinate, s , has arbitrary origin.⁷ We chose the N–F distance as our reaction coordinate since it behaves almost linearly, going to infinity at the reactants or products and reaching its minimum value in the region of the complex. Figure 1 shows a three-dimensional representation of PES-1997 using the fitted parameters of the final functional form. One notes the presence of a well going downhill toward the very exothermic exit channel.

Finally, note that this surface had only been used in kinetics studies,² for rate constant calculations and kinetic isotope effects, considering the temperature range 100–500 K, giving reasonable agreement with the experimental data that was then available.^{8–11} However, to the best of our knowledge, it has never been used in dynamics studies. The recent experimental study by Yang and co-workers¹ represents an excellent opportunity to further test the possibilities of this old, semiempirical surface.

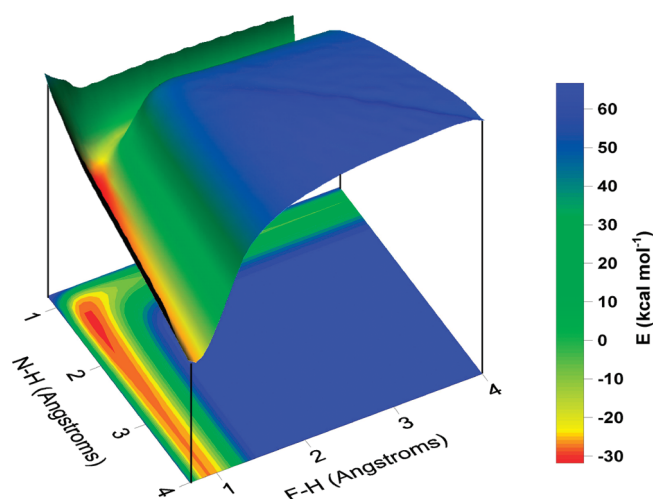


Figure 1. Three-dimensional representation of the PES of the gas-phase $F + \text{NH}_3$ reaction.

3. COMPUTATIONAL DETAILS

The QCT calculations^{12–14} were carried out using the VENUS96 code,¹⁵ customized to incorporate our analytical PES. The integration step was 0.01 fs, with an initial separation between the F atom and the ammonia center of mass of 6.0 Å. The vibrational and rotational energies were obtained by thermal sampling at 20 K from a Boltzmann distribution, with a reactant collision energy of 4.5 kcal mol^{−1} to simulate the crossed-beam experiments. The maximum value of the impact parameter, b_{max} was 4.2 Å. To compare experimental and theoretical QCT results, batches of 100 000 trajectories were calculated for each of the two reactions, NH_3 and ND_3 .

As usual in the VENUS code, the available final energy in the products is decomposed in relative translational and internal (sum of rotational and vibrational) energies. The relative translational energy is calculated from the relative momentum of the center of mass of the two products. The internal energy of each product is obtained from the sum of the respective potential and kinetic energies, which are available from the coordinates and momenta of each product at the end of the reactive trajectory. Then, the rotational energy for each product is calculated from their respective angular momenta, averaged over 200 steps, while the vibrational energy is obtained as the difference from the internal energy, assuming obviously the separation of the rotational–vibrational motions.

One of the major difficulties with quasi-classical simulations is the question of how to handle the zero-point energy (ZPE) problem. Various strategies have been proposed to correct this quantum-mechanical effect (refs 16–24, and references therein), but no really satisfactory alternatives have emerged. Here we employed a pragmatic solution, the so-called passive method,²¹ which consists in running the trajectories with no quantum constraint to subsequently analyze them and discard those that are not allowed in a quantum mechanical world, even though this method is known to perturb the statistics and can therefore lead to uncertainties in the dynamics study.²⁵ In particular, we discard all the trajectories for which either of the products has a vibrational energy lower than its harmonic ZPE. We call this histogram binning with double ZPE correction (HB-DZPE).

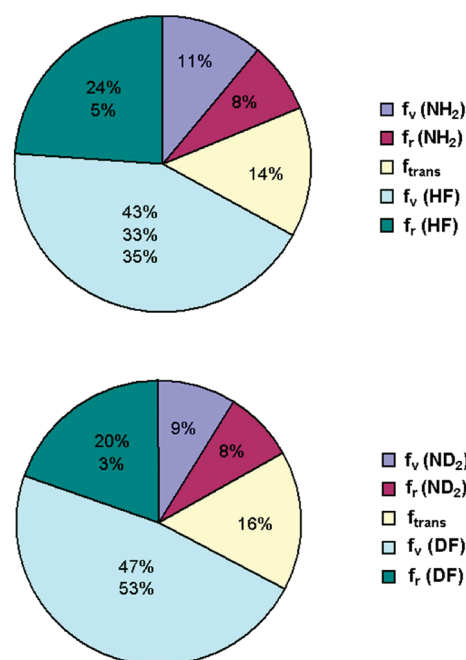


Figure 2. Product energy partitioning (percentages) (maximum error bar ± 1) for the $F + \text{NH}_3$ (top panel) and $F + \text{ND}_3$ (bottom panel) reactions at 4.5 kcal mol^{−1}. Where available, the first entry is the QCT result on the PES-1997 surface, the second entry the experimental data from ref 27, and the third entry the experimental data from ref 26.

4. RESULTS AND DISCUSSION

We shall begin by analyzing the product energy partitioning and the $\text{HF}(v')$ and $\text{DF}(v')$ product vibrational distribution, which have been reported experimentally.^{26–33} This comparison represents a severe test of the quality of the PES-1997. Figure 2 plots the QCT average product fraction of the energy in translation (f_{trans}), vibration (f_v), and rotation (f_r) of the products for the NH_3 and ND_3 reactions at 4.5 kcal mol^{−1}, together with the sparse experimental values^{26,27} for comparison. The QCT results show that the energy is released mainly as vibration in the diatomic product with a small internal energy in the polyatomic coproduct. They also show that a greater fraction of vibrational energy goes into the DF product than into the analogous HF product, in agreement with infrared chemiluminescence experiments.²⁷ The greatest discrepancy is found in the rotational distribution: 24% (20% for ND_3) vs the experimental data, 5% (3% for ND_3). This is probably due to an excessively attractive character of the stretching terms of the functional form describing the PES-1997, which favors rotational motion in the products. Consequently, the vibrational energy in the products will appear underestimated with respect to experiment, and a lower excitation vibrational of the HF product will be obtained using this surface.

The $\text{HF}(v')$ and $\text{DF}(v')$ QCT vibrational distributions are plotted in Figure 3, together with the available experimental data for comparison.³² The QCT calculations reproduce the experimental behavior, in which inverted distributions are found for the $\text{HF}(v'=1)$ and $\text{DF}(v'=2)$ products. This agreement of the theoretical results with the available experimental data lends credence to the PES-1997 surface.

Next, we analyze the product angular distribution, which is directly related to the recent crossed-beam experiment of Yang

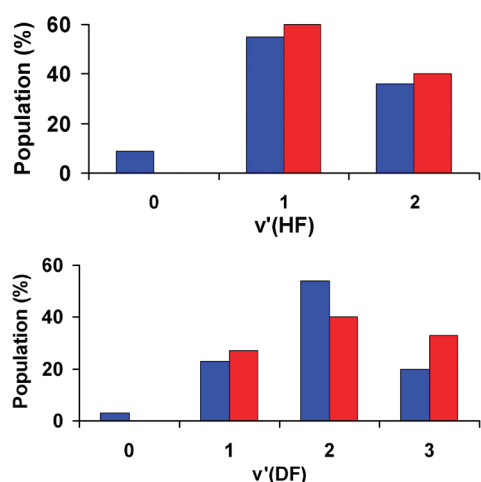


Figure 3. Vibrational populations for HF(v') in the F + NH₃ reaction (top panel) and for DF(v') in the F + ND₃ reaction (bottom panel). Experimental values²⁷ in red.

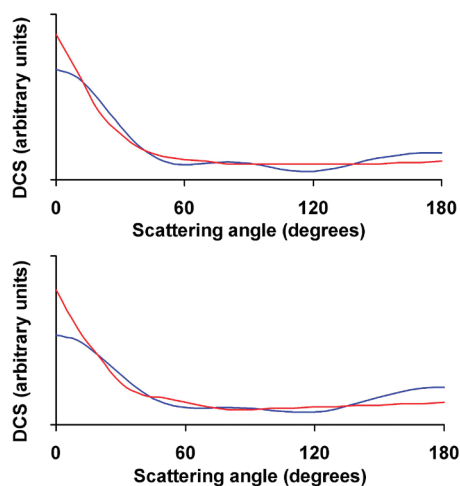


Figure 4. Product angular distributions for the HF(all v') product in the F + NH₃ reaction (top panel) and for the DF(all v') in the F + ND₃ reaction (bottom panel). The scattering distributions are normalized so that the area under the common regions is the same.

and co-workers. This property is doubtless one of the most sensitive dynamics features with which to test the quality of the PES. The QCT angular distributions of the HF and DF products with respect to the incident F atom (obtained as differential cross sections, DCSs) are plotted in Figure 4, together with the recent experimental data.¹ The F + NH₃ and the F + ND₃ reactions present similar behavior—mainly forward-scattered with a small sideways-backward contribution, reproducing the experimental data, although the theoretical values are slightly less forward. Also in agreement with experiment, the forward distribution is greater for the F + NH₃ reaction than for the F + ND₃ reaction.

The authors of the experimental study¹ conjectured, based also on earlier infrared chemiluminescence results,^{26,27} a mechanism involving competition between direct abstraction (responsible for the forward distribution) and the formation of a long-lived complex in the exit channel (responsible for the forward–backward distribution). They found it difficult, however, to separate

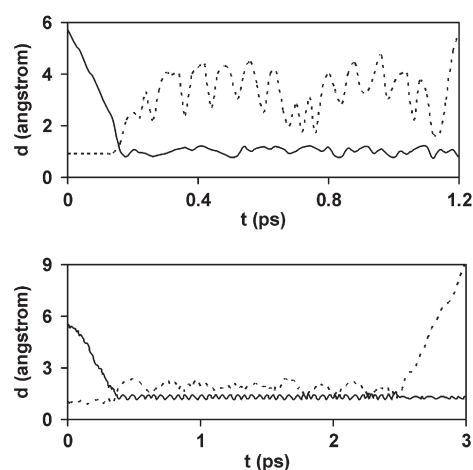


Figure 5. Representative plots of different reaction mechanisms for indirect trajectories, shown as the evolution of the N–H (dotted line) and H–F (solid line) distances as a function of time: a “nearly-trapped” trajectory with a “yo-yo” mechanism (top panel) and a typical long-lived complex formation mechanism (bottom panel, which corresponds to the Cl + NH₃ reaction).

the contributions of the different mechanisms. To look deeper into this issue, we analyzed the reactive trajectories individually. We found that about 90% are direct, i.e., unmodified by the presence of the deep well in the exit channel. They are associated with large impact parameters and are responsible for the observed forward distributions. This is the expected behavior for a barrierless reaction, where the collision energy is then relatively large, 4.5 kcal mol^{−1}. The remaining 10% of the trajectories are indirect, with a forward–backward symmetry. Because of the existence of the well in the exit channel, the system persists for some time, “forgetting” the initial approach direction, before the formation of the products. Obviously, when all the trajectories (direct and indirect) are considered, the angular distribution exhibits mainly forward symmetry.

What is the nature of these “indirect” trajectories? By individual visualization and animation of the indirect trajectories, we found that they are not due to long-lived complexes (understood as chemically bound systems which survive for at least a rotational period) caused by the presence of the well in the exit channel as had been suggested earlier but to a different mechanism. In particular, once the HF and NH₂ (or DF and ND₂) products have been formed, they do not fly apart from each other. Instead, they undergo several collisions in the exit channel associated with rotation of the diatomic product, before finally separating. Classically, these “nearly-trapped” trajectories are similar to the motion of a spring or a “yo-yo”. To better illustrate the difference between the two “indirect” trajectory mechanisms, Figure 5 plots the temporal evolution of the N–H bond, which is broken (dashed line), and the H–F bond, which is formed (solid line), for the “yo-yo” mechanism found in the present study (top panel) and for a textbook example of a long-lived complex (bottom panel). Note that this latter long-lived complex corresponds to the Cl + NH₃ hydrogen abstraction reaction. This has also been studied by our laboratory (unpublished results) and also presents a well in the exit channel; although unlike the present reaction, it is endothermic.

The periodicity observed in the top panel of Figure 5, dashed line, due to the continuous motions of approaching and retreating from the broken N–H bond, is associated with the rotation

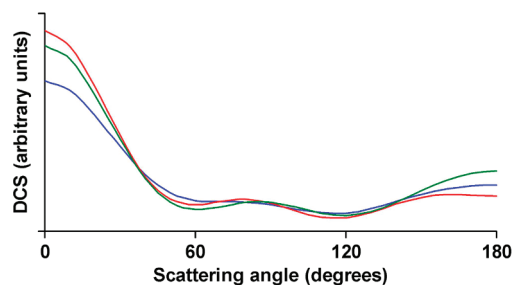


Figure 6. Product angular distributions for the $F + \text{NH}_3 \rightarrow \text{HF}(v') + \text{NH}_2$ reaction for different HF vibrational states. Note that, for the sake of clarity, the individual distributions have not been scaled to their respective percentages (9%, 55%, and 36% for $v' = 0, 1$, and 2 , respectively). Blue line, $v' = 0$; red line, $v' = 1$; green line, $v' = 2$.

of the FH molecule. However, this rotational period is overestimated by about a factor of 10 with respect to the “standard” rotational period, $T_r = 1/(2B.c) \approx 800$ fs, due probably to the overestimation observed in the rotational energy with respect to the experimental data -24% vs 5% (Figure 2).

Finally, the Yang and co-workers experiment¹ only reported results for the total of the $\text{HF}(v')$ and $\text{DF}(v')$ vibrational states, without differentiating vibrational levels. In the present work, we also calculated the individual scattering distribution per vibrational mode. Figure 6 plots these results for the $F + \text{NH}_3 \rightarrow \text{HF}(v') + \text{NH}_2$ reaction. In all cases ($v' = 0, 1$, and 2), the scattering distribution is mainly forward with a small sideways–backward contribution, reproducing the whole of the scattering data. Since the results for the $F + \text{ND}_3$ reaction were similar, they are not presented here.

5. CONCLUSIONS

In conclusion, the present theoretical calculation based on an analytical potential energy surface developed by our research group has reproduced the experimental data of the title reaction, has led to the proposal of a new mechanism, which explains the “indirect” trajectories responsible for the sideways–backward symmetry, giving their contribution to the total mechanism, and has distinguished for the first time the independent vibrational contribution to the total scattering angle. We hope that these results will stimulate further experimental and theoretical work on this difficult reaction.

AUTHOR INFORMATION

Corresponding Author

*E-mail: joaquin@unex.es.

ACKNOWLEDGMENT

This work was partially supported by the Junta de Extremadura, Spain, and FEDER (Project No. IB10001). M.M.P. thanks the Junta de Extremadura (Spain) for a scholarship.

REFERENCES

- (1) Xiao, G.; Shen, G.; Wang, X.; Fan, H.; Yang, X. *J. Phys. Chem. A* **2010**, *114*, 4520.
- (2) Espinosa-García, J.; Corchado, J. C. *J. Phys. Chem. A* **1997**, *101*, 7336.
- (3) Duchovic, R. J.; Hase, W. L.; Schlegel, B. J. *J. Phys. Chem.* **1984**, *88*, 1339.

- (4) Yang, M.; Corchado, J. C. *J. Chem. Phys.* **2007**, *126*, 214312.
- (5) Page, M.; McIver, J. W., Jr. *J. Chem. Phys.* **1988**, *88*, 922.
- (6) Page, M.; Doubleday, C.; McIver, J. W., Jr. *J. Chem. Phys.* **1990**, *93*, 5634.
- (7) Rai, S. N.; Truhlar, D. G. *J. Chem. Phys.* **1983**, *79*, 6046.
- (8) Wategaonkar, S.; Setser, D. W. *J. Chem. Phys.* **1987**, *86*, 4477.
- (9) Pollock, T. L.; Jones, W. E. *Can. J. Chem.* **1973**, *51*, 204.
- (10) Houston, P. L. *Adv. Chem. Phys.* **1982**, *47*, 625.
- (11) Fagerström, K.; Jodkowski, S. T.; Lund, A.; Ratajczak, E. *Chem. Phys. Lett.* **1995**, *236*, 103.
- (12) Porter, R. N.; Raff, L. M. In *Dynamics of Molecular Collisions*, part B; Miller, W. H., Ed.; Plenum Press: New York, 1976.
- (13) Truhlar, D. G.; Muckerman, J. T. In *Atom-molecules Collision Theory*; Bernstein, R. B., Ed.; Plenum Press: New York, 1979.
- (14) Raff, L. M.; Thompson, D. L. In *Theory of Chemical Reaction Dynamics*; Baer, M., Ed.; CRC Press: Boca Raton, 1985.
- (15) Hase, W. L.; Duchovic, R. J.; Hu, X.; Komornicki, A.; Lim, K. F.; Lu, D. h.; Peshherbe, G. H.; Swamy, K. N.; Vande Linde, S. R.; Varandas, A. J. C.; Wang, H.; Wolf, R. J. *VENUS96: A General Chemical Dynamics Computer Program*. *QCPE Bull.* **1996**, *43*.
- (16) S.F. Wu, S. F.; Marcus, R. A. *J. Phys. Chem.* **1970**, *53*, 4026.
- (17) Bowman, J. M.; Kuppermann, A. *J. Chem. Phys.* **1973**, *59*, 6524.
- (18) Truhlar, D. G. *J. Phys. Chem.* **1979**, *83*, 18.
- (19) Schatz, G. C. *J. Chem. Phys.* **1983**, *79*, 5386.
- (20) Lu, D. h.; Hase, W. L. *J. Chem. Phys.* **1988**, *89*, 6723.
- (21) Varandas, A. J. C. *Chem. Phys. Lett.* **1994**, *225*, 18.
- (22) Bonnet, L.; Rayez, J. C. *Chem. Phys. Lett.* **1997**, *277*, 183.
- (23) Marques, J. M. C.; Martínez-Núñez, E.; Fernández-Ramos, A.; Vazquez, S. J. *J. Phys. Chem.* **2005**, *109*, 5415.
- (24) Duchovic, R. J.; Parker, M. A. *J. Phys. Chem.* **2005**, *109*, 5883.
- (25) Guo, Y.; Thomson, D. L.; Sewell, T. D. *J. Chem. Phys.* **1996**, *104*, 576.
- (26) Douglas, D. J.; Sloan, J. J. *J. Chem. Phys.* **1980**, *46*, 307.
- (27) Sloan, J. J.; Watson, D. G.; Williamson, J. *Chem. Phys. Lett.* **1980**, *74*, 481.
- (28) Manocha, D. S.; Setser, D. W.; Wickramaaratchi, M. *Chem. Phys.* **1983**, *76*, 129.
- (29) Donaldson, D. J.; Parsons, J.; Sloan, J. J.; Stolow, A. *Chem. Phys.* **1984**, *85*, 47.
- (30) Donaldson, D. J.; Sloan, J. J.; Goddard, J. D. *J. Chem. Phys.* **1985**, *82*, 4524.
- (31) Wategaonkar, S.; Setser, D. W. *J. Chem. Phys.* **1987**, *86*, 4477.
- (32) Goddard, J. D.; Donaldson, D. J.; Sloan, J. J. *J. Chem. Phys.* **1987**, *114*, 321.
- (33) Sloan, J. J. *J. Phys. Chem.* **1988**, *92*, 18.